

Direct Observation of the Ion-Pair Dynamics at a Protein–DNA Interface by NMR Spectroscopy

Kurtis M. Anderson,^{†,‡} Alexandre Esadze,[†] Mariappan Manoharan,^{§,||} Rafael Brüschweiler,[§] David G. Gorenstein,[‡] and Junji Iwahara^{*,†}

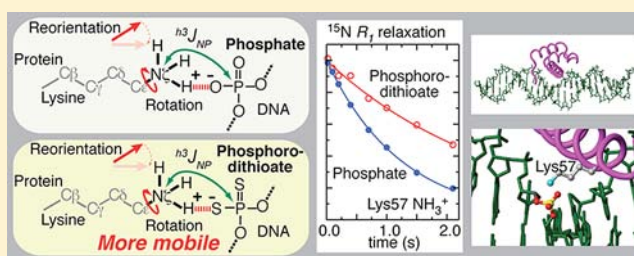
[†]Sealy Center for Structural Biology and Molecular Biophysics, Department of Biochemistry and Molecular Biology, University of Texas Medical Branch, Galveston, Texas 77555, United States

[‡]Department of NanoMedicine and Biomedical Engineering, Institute of Molecular Medicine, University of Texas Health Science Center at Houston, Houston, Texas 77030, United States

[§]Chemical Sciences Laboratory, Department of Chemistry and Biochemistry, and National High Magnetic Field Laboratory, Florida State University, Tallahassee, Florida 32306, United States

Supporting Information

ABSTRACT: Ion pairing is one of the most fundamental chemical interactions and is essential for molecular recognition by biological macromolecules. From an experimental standpoint, very little is known to date about ion-pair dynamics in biological macromolecular systems. Absorption, infrared, and Raman spectroscopic methods were previously used to characterize dynamic properties of ion pairs, but these methods can be applied only to small compounds. Here, using NMR ¹⁵N relaxation and hydrogen-bond scalar ¹⁵N–³¹P *J*-couplings (^{h3}*J*_{NP}), we have investigated the dynamics of the ion pairs between lysine side-chain NH₃⁺ amino groups and DNA phosphate groups at the molecular interface of the HoxD9 homeodomain–DNA complex. We have determined the order parameters and the correlation times for C–N bond rotation and reorientation of the lysine NH₃⁺ groups. Our data indicate that the NH₃⁺ groups in the intermolecular ion pairs are highly dynamic at the protein–DNA interface, which should lower the entropic costs for protein–DNA association. Judging from the C–N bond-rotation correlation times along with experimental and quantum-chemically derived ^{h3}*J*_{NP} hydrogen-bond scalar couplings, it seems that breakage of hydrogen bonds in the ion pairs occurs on a sub-nanosecond time scale. Interestingly, the oxygen-to-sulfur substitution in a DNA phosphate group was found to enhance the mobility of the NH₃⁺ group in the intermolecular ion pair. This can partially account for the affinity enhancement of the protein–DNA association by the oxygen-to-sulfur substitution, which is a previously observed but poorly understood phenomenon.



INTRODUCTION

Ion pairing is one of the most fundamental atomic interactions in both chemistry and biology. In solution, one distinguishes two major states of ion pairs: contact ion pairs (CIP) and solvent-separated ion pairs (SIP).^{1–4} In the CIP state, a cation and an anion are in direct contact with each other, whereas, in the SIP state, there are one or more solvent molecules between the electrostatically interacting cation and anion. In previous studies, ion-pair dynamics of small organic compounds were characterized experimentally using time-resolved absorption spectroscopy, infrared spectroscopy, and Raman spectroscopy.^{5–8} The transitions between the CIP and SIP states were found to occur on a picosecond to nanosecond time scale for the ion pairs of these small organic compounds, and the free energy differences between their CIP and SIP states were found to be ~1–2 kcal/mol.^{5–9} Despite the wealth of information available for small organic compounds, very little is currently known about the dynamics of ion pairs tethered to biological

macromolecules because their complexity renders application of the above-mentioned methods impractical.

The importance of ion pairs for protein function is evident from X-ray crystal structures. However, crystallographic data do not provide adequate information about dynamic properties of the ion pairs. For example, the presence of transitions between CIP and SIP states in macromolecules and their time scale are inaccessible by crystallography. Currently, ion-pair dynamics and its role in biological macromolecular systems is not understood by experimental means, which represents a bottleneck for understanding the relationship between structural dynamics and protein functions.

Here we present experimental data on ion-pair dynamics at protein–DNA interfaces. Formation of intermolecular ion pairs between protein and DNA along with release of counterions is the major driving force for many protein–DNA complexes

Received: December 17, 2012

Published: February 14, 2013

(e.g., reviewed in refs 10–12). Our current work is based on the NMR methods developed recently for lysine (Lys) side-chain NH_3^+ groups.^{13–17} By analyzing the ^{15}N relaxation of interfacial Lys NH_3^+ groups and hydrogen-bond scalar ^{15}N – ^{31}P couplings ($^hJ_{\text{NP}}$) across the ion pairs between protein and DNA, we probe the ion-pair dynamics at the molecular interface in the HoxD9 homeodomain–DNA complex. ^{15}N relaxation data provide motional information on reorientation and bond rotations of NH_3^+ groups,¹³ whereas $^hJ_{\text{NP}}$ data reflecting orbital overlaps in hydrogen bonds provide unique information on hydrogen bonding.^{18–21} In the current case, sizable $^hJ_{\text{NP}}$ couplings represent direct evidence for the CIP state of the intermolecular ion pairs. Owing to slower hydrogen exchange due to ion pairing, the NMR signals of the interfacial Lys side-chain NH_3^+ groups (Lys3, Lys55, and Lys57) in this complex can be clearly observed at 35 °C, a temperature at which signals from all the other NH_3^+ groups are broadened beyond detection.¹⁴ With this system, we demonstrate the highly dynamic nature of the interfacial ion pairs and discuss its biological significance. By comparing the ion-pair dynamics between normal phosphate ($-\text{O}-\text{PO}_2^--\text{O}-$) and phosphorodithioate ($-\text{O}-\text{PS}_2^--\text{O}-$) groups, this work also provides mechanistic insights into why the oxygen-to-sulfur substitution in DNA phosphate groups can enhance binding of proteins to DNA.^{22–26}

MATERIAL AND METHODS

Sample Preparation. $^2\text{H}/^{15}\text{N}$ -labeled HoxD9 homeodomain (with C6S mutation) and unlabeled 24-bp DNA duplex containing a target sequence (TAATGG) were prepared as described previously.^{27–29} The protein was mixed with the 24-bp DNA duplex at a molar ratio of 1:1.4 (DNA in excess). Unmodified DNA strands were purchased from Integrated DNA Technologies. The DNA strand containing a phosphorodithioate group was synthesized on an Expedite 8909 DNA synthesizer with standard dA/dC/dG/dT-phosphoramidites (Glen Research) and dC-thiophosphoramidite (AM Biotechnologies/Glen Research). After reverse-phase HPLC purification via a 5'-dimethoxytrityl group, ESI-MS analysis confirmed oligo identity and incorporation of both sulfur atoms. Duplexes for NMR were prepared by annealing complementary strands and purified via anion-exchange chromatography to remove minor single-stranded DNA excess due to the uncertainty in measuring single strand concentrations. For fluorescence measurements, the DNA strand with a 5'-amine-linked rhodamine was purchased from Midland Certified Reagents and the annealed fluorescent DNA duplexes were purified using polyacrylamide gel electrophoresis. A 280- μL solution of 1.0 mM HoxD9 homeodomain–DNA complex, 20 mM NaCl, and 20 mM sodium phosphate (pH 5.8) was sealed into an inner tube of coaxial NMR tube with D_2O separately sealed into the outer layer (to avoid isotopic isomers NDH_2^+ , ND_2H^+ , and ND_3^+).

NMR Experiments. NMR experiments were performed using Bruker Avance III 600-MHz and 800-MHz spectrometers equipped with cryogenic probes. All ^{15}N relaxation measurements were carried out at 35 °C. ^{15}N longitudinal and transverse relaxation and ^1H – ^{15}N heteronuclear NOE for Lys side-chain NH_3^+ groups were measured at ^1H frequencies of 600 and 800 MHz as described in our previous work.¹³ Order parameters S^2_{axis} , correlation times for C–N bond rotation, and reorientation of C–N bond were calculated from the relaxation data by nonlinear least-squares fitting as described previously.¹³ In the fitting procedure, the heteronuclear NOE was calculated using eq 17 rather than eq 16 in ref 13, because relaxation rates of $4N_zH_zH_z$ terms were found to be greater than 60 s^{-1} (which makes the two equations virtually identical). Uncertainties in calculated parameters were estimated with the Monte Carlo method. The effective rotational correlation time and diffusion anisotropy at 35 °C were determined from backbone ^{15}N R_1 and R_2 rates as described.³⁰ 2-D $\text{H}_3(\text{N})\text{P}$ spectra and 2-D spin-echo $^hJ_{\text{NP}}$ –

modulation constant-time HISQC spectra were recorded at 15 °C with a QCI ($^1\text{H}/^{13}\text{C}/^{15}\text{N}/^{31}\text{P}$) cryogenic probe at a ^1H frequency of 600 MHz. Other details on the $^hJ_{\text{NP}}$ analyses including DFT-based prediction are given in Supporting Information (SI).

Affinity Measurements for Homeodomain–DNA Association. Affinities of HoxD9 homeodomain for the two 24-bp target DNA duplexes I and II were determined using the fluorescence anisotropy as a function of protein concentration (0.1–800 nM). Fluorescence arising from rhodamine conjugated at a 5'-terminus of DNA (4 nM) was monitored using an ISS PC-1 spectrofluorometer. Excitation and emission wavelengths used were 555 and 588 nm, respectively. The titration experiments were performed three times at 20 °C using a buffer of 20 mM sodium acetate (pH 5.0) and 100 mM NaCl, in which aggregation of the free homeodomain was avoided.³¹

RESULTS

Mobility of Lys NH_3^+ Groups in Ion Pairs with DNA. In this work, the ion-pair dynamics at protein–DNA interface were investigated for two DNA complexes of HoxD9 homeodomain: One with a normal 24-bp DNA duplex (“Complex I”), the other with a modified 24-bp DNA duplex containing a phosphorodithioate group instead of the phosphate group that forms an ion pair with Lys57 (“Complex II”) (Figure 1a). In Lys-selective two-dimensional (2D) heteronuclear in-phase single quantum coherence (HISQC) spectra,¹⁴ ^1H – ^{15}N cross-peaks of side-chain NH_3^+ groups of Lys3, Lys55, and Lys57 were observed for both complexes at pH 5.8 and 35 °C. As shown in Figure 1, the oxygen-to-sulfur substitution in the ion pair with Lys57 caused large perturbations in ^1H and ^{15}N resonances of Lys57 NH_3^+ group ($|\Delta\delta_{\text{H}}|$, 0.21 ppm; and $|\Delta\delta_{\text{N}}|$, 0.78 ppm). Signals from Lys3 and Lys55 NH_3^+ groups remained almost unchanged, which is not surprising because the location of the dithioation is specifically on the phosphate group interacting with Lys57. For the Lys NH_3^+ groups of Complexes I and II, we measured ^{15}N relaxation rates R_1 , R_2 , and $R(4N_zH_zH_z)$ and ^1H – ^{15}N nuclear Overhauser enhancement (NOE) as described previously.¹³ From these relaxation data, we determined order parameters for the amino-group symmetry axis S^2_{axis} , C–N bond rotational correlation times τ_b , and reorientational correlation times τ_i for Lys NH_3^+ groups (Figure 2a). The results are summarized in Table 1. Interestingly, the order parameters S^2_{axis} of Lys NH_3^+ groups interacting DNA were relatively low (<0.5), indicating that the ion pairs between Lys side-chain NH_3^+ and DNA phosphate groups are highly mobile. In previous work on ubiquitin, we found that Lys side-chain NH_3^+ groups involved in a hydrogen bond had order parameters $S^2_{\text{axis}} < 0.5$, an observation consistent with 1- μs molecular dynamics simulations.¹³ Although one may expect that the hydrogen-bonding and short-range electrostatic interactions in ion pairs may cause a higher degree of motional restriction, our data indicate that the ion pairs between protein and DNA are remarkably dynamic. The dynamic nature of the interfacial ion pairs should be favorable for protein–DNA association because it should minimize the loss of conformational entropy from immobilization of side chains upon the formation of the complex.

Direct Evidence for the CIP State. To obtain information on the CIP and SIP states, we studied hydrogen-bond scalar couplings $^hJ_{\text{NP}}$ between Lys side-chain ^{15}N and DNA ^{31}P nuclei in the ion pairs at the protein–DNA interface. Note that the CIP state can exhibit $^hJ_{\text{NP}}$ coupling whereas the SIP state cannot (Figure 2b). We designed the 2-D heteronuclear correlation $\text{H}_3(\text{N})\text{P}$ experiment (the pulse sequence shown in Figure S1A) for observing the signals arising from coherence

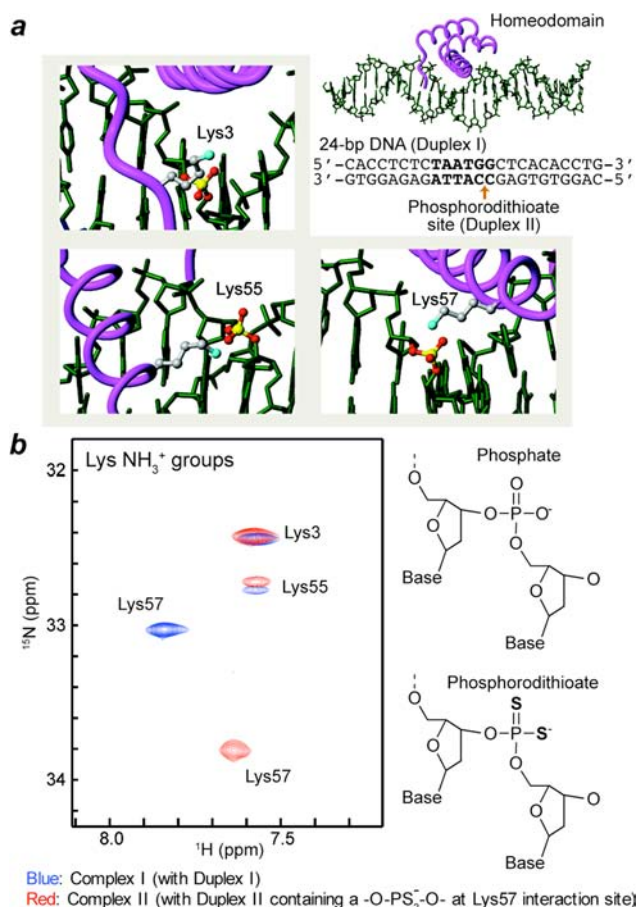


Figure 1. (a) Intermolecular ion pairs involving Lys side-chain NH_3^+ groups (cyan spheres) and DNA phosphate groups (yellow/red spheres) studied in this work. Two 24-bp DNA duplexes with the same sequence (the recognition site in bold) were used: Duplex I with no chemical modification; and Duplex II with a phosphorodithioate incorporated at the position of the ion pair with Lys57. (b) Overlaid HISQC spectra of the Lys NH_3^+ groups recorded for HoxD9 homeodomain complexes with Duplex I (blue) and with Duplex II (red) at 35 °C.

transfer via $^3\text{J}_{\text{NP}}$ coupling. Despite the small magnitude of this type of coupling (<1 Hz), the very slow ^{15}N transverse relaxation of NH_3^+ groups allowed us to observe the intermolecular correlation signals arising from $^3\text{J}_{\text{NP}}$ evolution by using relatively long periods for the coherence transfer.¹⁷ However, ^{31}P longitudinal relaxation in the form of scalar relaxation of the second kind³² for $2N_xP_z$ and $2N_yP_z$ terms during the periods renders an additional loss in sensitivity (an effect akin to those described by Bax and co-workers^{33,34}), which was estimated to be up to 10% in the current case (see SI for additional information). Spectra recorded by this experiment for Complexes I and II clearly show intermolecular ^1H - ^{31}P correlation signals (Figure 3a–c), indicating at least part-time presence of the CIP states for the ion pairs between Lys NH_3^+ and DNA phosphate/phosphorodithioate groups. Observed ^{31}P chemical shifts for DNA phosphates in the ion pairs with Lys55 (–4.88 ppm) and Lys57 (–3.86 ppm) lie at the outer edges of typical ^{31}P chemical shifts (–4.8 to –3.9 ppm) for B-form DNA,³⁵ presumably due to ion-pairing effects. ^{31}P chemical shift of the phosphorodithioate group in the ion pair with Lys57 was found to be 117.78 ppm (Figure 3c), which was confirmed with 1D ^{31}P NMR (Figure 3g).

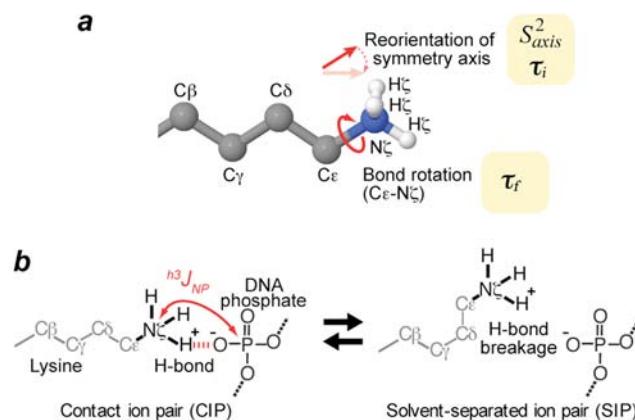


Figure 2. Ion-pair dynamics involving Lys NH_3^+ and DNA phosphate group. (a) Reorientation of symmetry axis and C–N bond rotation studied by ^{15}N relaxation for Lys side-chain NH_3^+ group. Determined values of the parameters describing these motions are shown in Table 1. Based on the almost ideal tetrahedral geometry found for NH_3^+ groups,⁵² the order parameter for bond rotation was assumed to be 0.111.¹³ (b) Transitions between CIP and SIP states of intermolecular ion pairs. $^3\text{J}_{\text{NP}}$ coupling is present only for the CIP.

To determine the absolute values of $^3\text{J}_{\text{NP}}$ coupling constants, we designed the spin-echo $^3\text{J}_{\text{NP}}$ -modulation constant-time HISQC experiment (the pulse sequence shown in Figure S1B). Using signal intensities in the two sub-spectra recorded by this experiment, we determined the absolute values of the $^3\text{J}_{\text{NP}}$ coupling constants for the intermolecular ion pairs in Complex I and II to range from 0.06 to 0.63 Hz (Figure 3d–f). The measured $^3\text{J}_{\text{NP}}$ constants are biased toward smaller values due to the partial self-decoupling effect³⁶ arising from ^{31}P longitudinal relaxation. But this effect can readily be corrected as described in SI. Differences between original and corrected values are less than 0.05 Hz. For Lys55 and Lys57 NH_3^+ groups, crystal structures of highly homologous protein–DNA complexes exhibit the CIP states of their ion pairs with DNA. For these NH_3^+ groups, we also predicted $^3\text{J}_{\text{NP}}$ coupling constants from the crystal structures by density functional theory (DFT) method as described previously.¹⁸ The results of the DFT calculations are given in Table S1. As shown in previous DFT studies (reviewed in ref 19), a hydrogen-bond scalar coupling is highly sensitive to subtle differences in hydrogen-bonding geometry. This complicates the quantitative assessment of ion-pair dynamics accompanying geometrical change of hydrogen bonds. In fact, a large variation was found in $^3\text{J}_{\text{NP}}$ constants predicted from different crystal structures (Table S1). Nonetheless, the experimental $^3\text{J}_{\text{NP}}$ constants were comparable to the averages of the predicted constants, suggesting that the CIP state has a major presence in solution for the ion pairs of Lys55 and Lys57 NH_3^+ groups with a DNA phosphate group. The $^3\text{J}_{\text{NP}}$ coupling for phosphorodithioate–Lys57 NH_3^+ ion pair (0.18 Hz) was found to be significantly smaller than that for phosphate–Lys57 NH_3^+ ion pair (0.33 Hz). In contrast, DFT calculations suggested that $|^3\text{J}_{\text{NP}}|$ of phosphorodithioate tends to be larger for the same hydrogen-bonding geometry (see Tables S1 and S2). The observed small $|^3\text{J}_{\text{NP}}|$ for the phosphorodithioate–Lys57 NH_3^+ ion pair could be partly due to the higher degree of dynamics that our ^{15}N relaxation data indicate (see below).

Hydrogen-Bonding Dynamics of the Intermolecular Ion Pairs. Our experimental and computational $^3\text{J}_{\text{NP}}$ coupling data suggest a major presence of CIP for the intermolecular ion

Table 1. ^{15}N Relaxation and Dynamics Parameters for the Lys Side-Chain NH_3^+ Groups in the Intermolecular Ion Pairs in the HoxD9 Homeodomain–DNA Complexes at 35 °C

| | Complex I ^a | | | Complex II ^b | | |
|---|------------------------|-----------------------|-----------------------|-------------------------|-----------------------|-----------------------|
| | Lys3 NH_3^+ | Lys55 NH_3^+ | Lys57 NH_3^+ | Lys3 NH_3^+ | Lys55 NH_3^+ | Lys57 NH_3^+ |
| 800 MHz | | | | | | |
| ^{15}N R_1 (s^{-1}) | 0.25 ± 0.01 | 0.43 ± 0.02 | 0.74 ± 0.01 | 0.29 ± 0.02 | 0.43 ± 0.03 | 0.33 ± 0.02 |
| ^{15}N $R_{2,\text{ini}}$ (s^{-1}) ^c | 0.98 ± 0.05 | 1.98 ± 0.21 | 2.27 ± 0.04 | 1.16 ± 0.07 | 2.18 ± 0.26 | 1.76 ± 0.05 |
| ^1H – ^{15}N NOE | –2.40 ± 0.03 | –2.72 ± 0.08 | –3.00 ± 0.03 | –2.63 ± 0.06 | –2.72 ± 0.09 | –3.02 ± 0.13 |
| 600 MHz | | | | | | |
| ^{15}N R_1 (s^{-1}) | 0.27 ± 0.01 | 0.59 ± 0.04 | 0.80 ± 0.02 | 0.29 ± 0.02 | 0.54 ± 0.08 | 0.36 ± 0.02 |
| ^1H – ^{15}N NOE | –3.07 ± 0.06 | –2.94 ± 0.17 | –3.17 ± 0.04 | –3.24 ± 0.10 | –3.08 ± 0.20 | –3.08 ± 0.13 |
| Dynamics ^d | | | | | | |
| S^2_{axis} | 0.22 ± 0.02 | 0.46 ± 0.06 | 0.48 ± 0.01 | 0.26 ± 0.02 | 0.49 ± 0.06 | 0.39 ± 0.01 |
| τ_f (ps) | 3 ± 1 | 23 ± 2 | 113 ± 42 | 8 ± 4 | 26 ± 12 | 27 ± 7 |
| τ_i (ps) | 222 ± 16 | 249 ± 42 | 82 ± 132 | 163 ± 43 | 184 ± 87 | 36 ± 19 |

^aWith Duplex I (see Figure 1). ^bWith Duplex II that contains a phosphorodithioate group at the ion pair with Lys57. ^cThe initial rate for intrinsically biexponential ^{15}N transverse relaxation¹³ of NH_3^+ . ^dSymbols are defined in Figure 2a. The molecular rotational correlation time and anisotropy were determined to be 10.6 ns and 2.1, respectively, from backbone ^{15}N relaxation data.

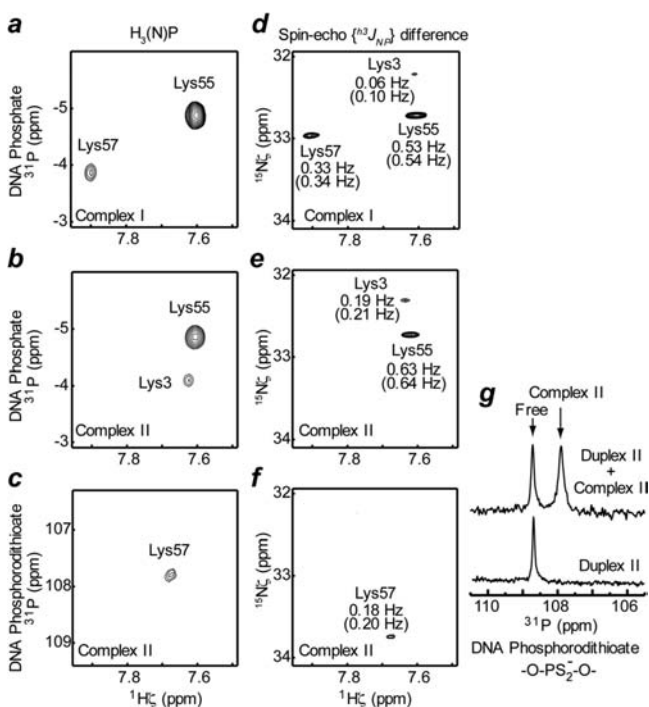


Figure 3. Hydrogen-bond scalar ^{15}N – ^{31}P coupling $^{h^3}J_{\text{NP}}$ between ^{15}N and ^{31}P nuclei as evidence for the presence of CIP. (a–c) 2D ^1H – ^{15}N P spectra that give heteronuclear ^1H – ^{31}P correlation cross peaks via $^{h^3}J_{\text{NP}}$ coupling. ^{31}P chemical shifts are relative to trimethylphosphate (TMP). (d–f) Difference spectra recorded by the spin–echo $^{h^3}J_{\text{NP}}$ –modulation constant-time HISQC experiment. Measured absolute values of $^{h^3}J_{\text{NP}}$ are also indicated. Percentage errors were estimated to be less than 20%. Values in parentheses are $^{h^3}J_{\text{NP}}$ values taking account of the correction due to partial self-decoupling arising from ^{31}P longitudinal relaxation (see S1). ^{31}P carrier positions were set to –3 ppm for panels a, b, d, and e (for DNA phosphate); and 107 ppm for panels c and f (for DNA phosphorodithioate). Spectra in panels a and d were recorded for Complex I, and spectra in panels b, c, e, and f for Complex II. The pulse sequences and other relevant details are given in Figure S1. (g) Phosphorodithioate regions of 1D ^{31}P spectra recorded for Duplex II in the free state and a mixture of Duplex II and Complex II. ^{31}P chemical shift of the cross peak in the panel c agrees with ^{31}P chemical shift of the signal from Complex II in panel g.

pairs involving Lys55 and Lys57 NH_3^+ groups. This is consistent with our finding that C–N bond-rotation correlation times τ_f of these NH_3^+ groups are clearly slower than that of Lys3 NH_3^+ group (Table 1). Hydrogen bonds with phosphate/phosphorodithioate in the CIP state should render slower bond rotations of Lys55 and Lys57 NH_3^+ groups. Transient breakage of the hydrogen bonds can be accompanied by rotational permutations of hydrogen atoms within the CIP state or a transition to SIP. Given the major presence of CIP, it is likely that the time scale of the transient hydrogen-bond breakage for Lys55 and Lys57 NH_3^+ groups is faster than or comparable to their bond-rotation correlation times τ_f . In fact, such a relation between τ_f and hydrogen-bonding lifetimes for Lys NH_3^+ groups in ubiquitin was previously found in molecular dynamics simulations.¹³ The τ_f and τ_i data in the current study suggest that the transient breakage of hydrogen bonds between Lys NH_3^+ and DNA phosphate/phosphorodithioate groups occurs on a subnanosecond time scale.

The faster C–N bond rotation of Lys3 NH_3^+ group implicates a higher population of the SIP state with no hydrogen bonds with DNA. The τ_f values for Lys3 NH_3^+ group in Complexes I and II are smaller than those (~25 ps) for Lys NH_3^+ groups that do not form any hydrogen bond in ubiquitin at 2 °C,¹³ but the higher temperature (35 °C) in the current study can explain this discrepancy. The Lys3 side chain is disordered in all of the crystal structures of homeodomain–DNA complexes except one (PDB 1IG7). The only structure available for the Lys3 side chain shows that the ion pair between Lys3 and DNA is in the SIP state with an $\text{N}\zeta\cdots\text{OP}$ distance of 5.4 Å, although simple rotation about χ_3 can reduce this distance to ~3.0 Å. On the other hand, weak $^{h^3}J_{\text{NP}}$ coupling was observed for Lys3 (Figures 3b, 3d and 3e), which indicates at least a part-time presence of the CIP. The small $^{h^3}J_{\text{NP}}$, short τ_f , and small S^2_{axis} collectively suggest a low population of the CIP state for the ion pair of Lys3 NH_3^+ group. Thus the equilibrium between the CIP and SIP states (Figure 2b) for Lys3 appears to be shifted toward the SIP, while the corresponding equilibria for Lys55 and Lys57 appear to be shifted toward the CIP.

Impact of Oxygen-to-Sulfur Substitution on Ion-Pair Dynamics. Our S^2_{axis} data indicate that Lys57 NH_3^+ group in the ion pair with a phosphorodithioate group is more mobile than in the ion pair with a phosphate group (Table 1). The

higher mobility is consistent with the two facts that (1) the effective ionic radius of sulfur (1.84 Å) is substantially larger than that of oxygen (1.40 Å), and (2) the potential energy surface for an H··S hydrogen bond is flatter than that for an H··O hydrogen bond.³⁷ Due to the flatter energy surface, on which a slight deviation from ideal hydrogen-bond geometry causes only a marginal increase in enthalpy, a donor of a H··S hydrogen bond should be able to take up a wider space without significant enthalpic loss. Order parameters for fixed-length bond vectors provide information only on orientational distributions, but do not provide the breadth of positional distributions or any information on translational motions.³⁸ By assuming a motional model for the bond vectors, however, qualitative information on conformational entropy can be obtained from such order parameters.^{39–42} Although the entropy for a whole side chain can be empirically estimated for relatively short amino acid side chains from order parameters measured only at the tip of the side chain, such relationships are less well-defined for longer amino acid side chains such as lysine and arginine.^{40,43} Based on the experimental order parameters S_{axis}^2 for Lys57 NH₃⁺ groups in Complexes I and II along with Yang and Kay's equation for the diffusion-in-a-cone model (i.e., entropic difference equals $k_B \ln\{[3 - (1 + 8S_{\text{axis,a}})^{1/2}]/[3 - (1 + 8S_{\text{axis,b}})^{1/2}]\}$, where k_B is the Boltzmann constant),⁴² the increase in entropy for the symmetry axis of the NH₃⁺ group by the oxygen-to-sulfur substitution was estimated to be 0.4 cal mol⁻¹ K⁻¹. We should mention that this is a rather crude estimate because the diffusion-in-a-cone model is likely to be too simplistic for the ion pairs undergoing the CIP-SIP transitions. Interestingly, the C–N bond rotation correlation time τ_f is significantly faster for Lys57 NH₃⁺ group in the ion pair with a phosphorodithioate group. This causes substantially different ¹⁵N R_1 rates of Lys57 NH₃⁺ groups in Complexes I and II (Figure 4a; see also Table 1). As considered previously for CH₃ groups,⁴⁴ the rotational entropy (S_{rot}) of an NH₃⁺ group is indirectly related to the bond rotation kinetics because the probability distribution function for rotation depends on the energy barrier for rotation. Provided that the Eyring equation in transition-state theory is applicable to NH₃⁺ rotation, experimental τ_f data along with the analytical expression⁴⁴ of S_{rot} suggest that NH₃⁺ rotational entropy increases by 0.4 cal mol⁻¹ K⁻¹ upon oxygen-to-sulfur substitution in the interacting DNA phosphate group. The overall increase of entropy (i.e., reorientational + rotational) by mobilizing the NH₃⁺ group is thus estimated to be ~0.8 cal mol⁻¹ K⁻¹.

This mobilization of the ion pair can at least partially account for affinity enhancement of the protein–DNA association by the oxygen-to-sulfur substitution. The affinity of Duplex II was found to be 3-fold higher than that of Duplex I (Figure 4b). By fluorescence anisotropy-based titration experiments, the dissociation constants (K_d) were determined to be 31 ± 6 nM for Complex I and 12 ± 4 nM for Complex II. From the K_d data, the difference between the binding free energies ($\Delta\Delta G = \Delta G_{\text{II}} - \Delta G_{\text{I}}$) is calculated to be -0.6 kcal/mol. The major contributor to this $\Delta\Delta G$ should be the entropy term (i.e., $-T\Delta\Delta S$), because recent theoretical quantum chemical studies showed that the enthalpy ΔH for H··S hydrogen bonds is slightly smaller than that for H··O hydrogen bonds.^{37,45} In fact, the entropic term for mobilization of the NH₃⁺ group alone corresponds to -0.24 kcal/mol at 20 °C. If the entropic effect for the other parts of the ion pair (e.g., methylene groups of the Lys side chain) is comparable to this, the observed $\Delta\Delta G$ can be

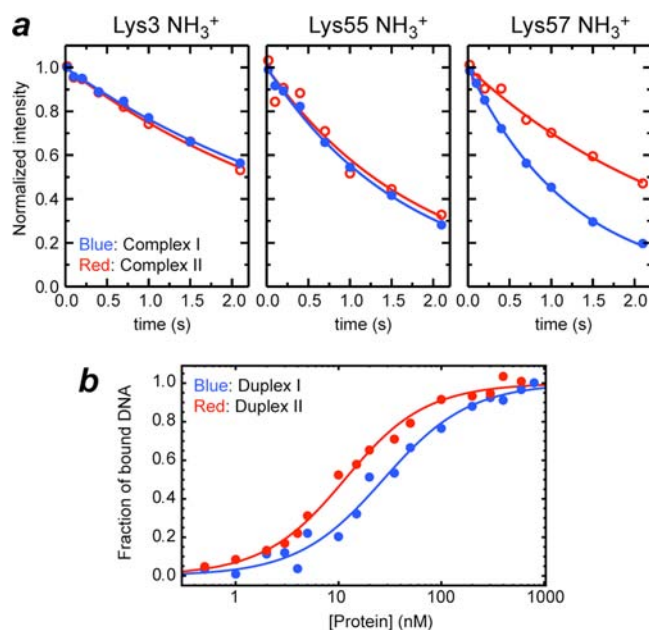


Figure 4. Influence of the oxygen-to-sulfur substitution in the DNA phosphate group interacting with Lys57. (a) ¹⁵N longitudinal relaxation of Lys side-chain NH₃⁺ groups at the protein–DNA interfaces of Complexes I and II. Lys57 NH₃⁺ group exhibited substantially different relaxation upon the oxygen-to-sulfur substitution in the DNA phosphate group. ¹⁵N relaxation of the other NH₃⁺ groups (interacting with normal phosphate group in both complexes) was virtually unaffected. (b) Binding isotherm as monitored with fluorescence arising from a rhodamine attached to the 5'-terminus of DNA. Fractions of bound DNA calculated from the fluorescence anisotropy data at varying concentrations of HoxD9 homeodomain are plotted for Duplexes I and II.

explained in terms of the enhanced ion-pair dynamics, though other factors (e.g., different desolvation energies) may also contribute.

DISCUSSION

Based on the counterion-condensation theory,^{46,47} macroscopic effects of counterion release due to ion pairing between protein and DNA were extensively studied by thermodynamic means in previous studies (e.g., reviewed in refs 10–12). On the other hand, the entropic effects for intermolecular ion pairs between protein side-chain and DNA phosphate groups was previously unknown by experimental means. Our experimental data on the ion-pair dynamics at the protein–DNA interface suggest that the entropic loss for basic side chains upon ion-pair formation is relatively small owing to remaining mobility as observed for the NH₃⁺ groups in the ion pairs with DNA. Comparison of our results for Complexes I and II suggests that modulation of the ion-pair dynamics can directly impact binding affinity. It is worth mentioning that the importance of remaining mobility of DNA phosphate groups in protein–DNA recognition was suggested based on 1-D ³¹P NMR data two decades ago.⁴⁸ The ion-pair dynamics seems entropically important for protein–DNA association.

The highly dynamic nature of the ion pairs between protein and DNA may also be kinetically advantageous. Due to extremely high DNA concentration in the nucleus and micromolar affinity for nonspecific DNA, transcription factors are mostly bound to nonspecific sites on chromosomal DNA in the search process before reaching their target DNA sites *in*

in vivo. In the case of the homeodomain, the structures of the nonspecific DNA complexes are very similar to that of the specific DNA complex.^{27,49} A nonspecific complex may form up to 6 CIPs involving Lys and Arg side chains as seen in crystal structures of the specific complexes. All CIPs with DNA need to be broken each time the protein moves from one nonspecific DNA site to another. Rapid CIP-SIP transitions should shorten the time necessary to break all CIPs, and thereby may facilitate the protein's sliding on nonspecific DNA and to efficiently locate the target sites. If the mean lifetime of CIP is $\sim 10^{-10}$ s and the population of SIP is $\sim 10\%$ (which corresponds to ~ 1.4 kcal/mol for a free energy difference between CIP and SIP, a reasonable value for small organic compounds⁵⁻⁹) for each ion pair, the time necessary for all 6 CIPs simultaneously to be broken is estimated to be $\sim 10^{-5}$ s. This is compatible with the time scale of proteins' sliding on DNA. One-dimensional diffusion coefficients for the sliding process, which were directly observed by single-molecule techniques,^{50,51} are typically between 10^{-3} and $10^{-1} \mu\text{m}^2 \text{s}^{-1}$. These data, together with a distance of 3.4 Å along the DNA axis for each sliding step from a nonspecific DNA site to an adjacent site, suggest that the mean times for individual sliding steps are in the range of 10^{-6} – 10^{-4} s.

CONCLUSION

Our present work provides the first experiment-based perspective of the ion-pair dynamics in a biological macromolecular system. Despite the simultaneous presence of the short-range electrostatic interaction and hydrogen bonding, the ion pairs between protein and DNA are highly dynamic on the sub-nanosecond time scale. The bond-rotation and reorientation correlation times suggest that breakage of hydrogen bonds in the CIP states of Lys NH_3^+ -phosphate/phosphorodithioate ion pairs occurs on a sub-nanosecond time scale. The high degree of flexibility of the intermolecular ion pairs, as reflected in the low order parameters of the Lys side chain cations, should minimize the side-chain conformational entropic costs for protein-DNA association. The oxygen-to-sulfur substitution in DNA phosphate makes the intermolecular ion pair more dynamic, which seems to contribute to the affinity enhancement by this type of substitution. The experimental data on the ion-pair dynamics in the relatively small protein-DNA complex may allow the computational biology community to validate and even improve the molecular dynamics protocols and force fields relevant for the simulation of ion pairs. This may ultimately lead to advances in the engineering of proteins that target specific DNA/RNA binding sites, the design of oligonucleotide-based scaffold structures, and the improvement of *in silico* screening of drugs involving ion pairs.

ASSOCIATED CONTENT

Supporting Information

NMR pulse sequences used for investigating hydrogen-bond coupling constants $^hJ_{\text{NP}}$ for lysine NH_3^+ -DNA phosphate/phosphorodithioate ion pairs; effect of ^{31}P longitudinal relaxation on $^hJ_{\text{NP}}$ coupling analysis; and DFT-based prediction of $^hJ_{\text{NP}}$ constants from crystal structures. This material is available free of charge via the Internet at <http://pubs.acs.org>.

AUTHOR INFORMATION

Corresponding Author

j.iwahara@utmb.edu

Present Address

^{||}School of Science, Engineering and Mathematics, Bethune-Cookman University, Daytona Beach, FL 32114

Notes

The authors declare no competing financial interest.

ACKNOWLEDGMENTS

This work was supported by Grants MCB-0920238 (to J.I.) and MCB-0918362 (to R.B.) from the National Science Foundation and by Grant 12BGIA8960032 from the American Heart Association (to J.I.). Additional support was provided by the Welch Foundation (AU-1296), National Cancer Institute (U54CA151668), and National Heart Lung and Blood Institute (HHSN268201000037C to D.G.G.). We thank Dr. Tianzhi Wang for technical support of UTMB's NMR instruments, and Drs. Montgomery Pettitt, James Stivers, David Volk, and John Ladbury for useful discussion.

REFERENCES

- (1) Collins, K. D. *Biophys. J.* **1997**, *72*, 65.
- (2) Macchioni, A. *Chem. Rev.* **2005**, *105*, 2039.
- (3) Marcus, Y.; Hefter, G. *Chem. Rev.* **2006**, *106*, 4585.
- (4) Szwarc, M. *Acc. Chem. Res.* **1969**, *2*, 87.
- (5) Simon, J. D.; Peters, K. S. *J. Am. Chem. Soc.* **1982**, *104*, 6542.
- (6) Masnovi, J. M.; Kochi, J. K. *J. Am. Chem. Soc.* **1985**, *107*, 7880.
- (7) Yabe, T.; Kochi, J. K. *J. Am. Chem. Soc.* **1992**, *114*, 4491.
- (8) Peters, K. S.; Li, B. L. *J. Phys. Chem.* **1994**, *98*, 401.
- (9) Lü, J. M.; Rosokha, S. V.; Lindeman, S. V.; Neretin, I. S.; Kochi, J. K. *J. Am. Chem. Soc.* **2005**, *127*, 1797.
- (10) Record, M. T., Jr.; Ha, J. H.; Fisher, M. A. *Methods Enzymol.* **1991**, *208*, 291.
- (11) Record, M. T., Jr.; Zhang, W.; Anderson, C. F. *Adv. Protein Chem.* **1998**, *51*, 281.
- (12) Privalov, P. L.; Dragan, A. I.; Crane-Robinson, C. *Nucleic Acids Res.* **2011**, *39*, 2483.
- (13) Esadze, A.; Li, D. W.; Wang, T.; Brüschweiler, R.; Iwahara, J. *J. Am. Chem. Soc.* **2011**, *133*, 909.
- (14) Iwahara, J.; Jung, Y. S.; Clore, G. M. *J. Am. Chem. Soc.* **2007**, *129*, 2971.
- (15) Takayama, Y.; Castañeda, C. A.; Chimenti, M.; García-Moreno, B.; Iwahara, J. *J. Am. Chem. Soc.* **2008**, *130*, 6714.
- (16) Takayama, Y.; Sahu, D.; Iwahara, J. *J. Magn. Reson.* **2008**, *194*, 313.
- (17) Zandarashvili, L.; Li, D. W.; Wang, T.; Brüschweiler, R.; Iwahara, J. *J. Am. Chem. Soc.* **2011**, *133*, 9192.
- (18) Czernek, J.; Brüschweiler, R. *J. Am. Chem. Soc.* **2001**, *123*, 11079.
- (19) Grzesiek, S.; Cordier, F.; Jaravine, V.; Barfield, M. *Prog. NMR Spectrosc.* **2004**, *45*, 275.
- (20) Löhr, F.; Mayhew, S. G.; Rüterjans, H. *J. Am. Chem. Soc.* **2000**, *122*, 9289.
- (21) Mishima, M.; Hatanaka, M.; Yokoyama, S.; Ikegami, T.; Walchli, M.; Ito, Y.; Shirakawa, M. *J. Am. Chem. Soc.* **2000**, *122*, 5883.
- (22) Cummins, L.; Graff, D.; Beaton, G.; Marshall, W. S.; Caruthers, M. H. *Biochemistry* **1996**, *35*, 8734.
- (23) King, D. J.; Ventura, D. A.; Brasier, A. R.; Gorenstein, D. G. *Biochemistry* **1998**, *37*, 16489.
- (24) King, D. J.; Bassett, S. E.; Li, X.; Fennwald, S. A.; Herzog, N. K.; Luxon, B. A.; Shope, R.; Gorenstein, D. G. *Biochemistry* **2002**, *41*, 9696.
- (25) Marshall, W. S.; Caruthers, M. H. *Science* **1993**, *259*, 1564.
- (26) Yang, X.; Bassett, S. E.; Li, X.; Luxon, B. A.; Herzog, N. K.; Shope, R. E.; Aronson, J.; Prow, T. W.; Leary, J. F.; Kirby, R.; Ellington, A. D.; Gorenstein, D. G. *Nucleic Acids Res.* **2002**, *30*, e132.
- (27) Iwahara, J.; Clore, G. M. *Nature* **2006**, *440*, 1227.
- (28) Iwahara, J.; Clore, G. M. *J. Am. Chem. Soc.* **2006**, *128*, 404.
- (29) Sahu, D.; Clore, G. M.; Iwahara, J. *J. Am. Chem. Soc.* **2007**, *129*, 13232.

- (30) Tjandra, N.; Feller, S. E.; Pastor, R. W.; Bax, A. *J. Am. Chem. Soc.* **1995**, *117*, 12562.
- (31) Dragan, A. I.; Li, Z.; Makeyeva, E. N.; Milgotina, E. I.; Liu, Y.; Crane-Robinson, C.; Privalov, P. L. *Biochemistry* **2006**, *45*, 141.
- (32) Abragam, A. *The Principle of Nuclear Magnetism*; Clarendon Press: Oxford, 1961; p 264.
- (33) Kuboniwa, H.; Grzesiek, S.; Delaglio, F.; Bax, A. *J. Biomol. NMR* **1994**, *4*, 871.
- (34) Vuister, G. W.; Bax, A. *J. Am. Chem. Soc.* **1993**, *115*, 7772.
- (35) Gorenstein, D. G. *Chem. Rev.* **1994**, *94*, 1315.
- (36) Harbison, G. S. *J. Am. Chem. Soc.* **1993**, *115*, 3026.
- (37) Wennmohs, F.; Staemmler, V.; Schindler, M. *J. Chem. Phys.* **2003**, *119*, 3208.
- (38) Iwahara, J.; Clore, G. M. *J. Am. Chem. Soc.* **2010**, *132*, 13346.
- (39) Akke, M.; Brüschweiler, R.; Palmer, A. G. *J. Am. Chem. Soc.* **1993**, *115*, 9832.
- (40) Li, D. W.; Brüschweiler, R. *J. Am. Chem. Soc.* **2009**, *131*, 7226.
- (41) Li, Z. G.; Raychaudhuri, S.; Wand, A. J. *Protein Sci.* **1996**, *5*, 2647.
- (42) Yang, D. W.; Kay, L. E. *J. Mol. Biol.* **1996**, *263*, 369.
- (43) Trbovic, N.; Cho, J. H.; Abel, R.; Friesner, R. A.; Rance, M.; Palmer, A. G., III *J. Am. Chem. Soc.* **2009**, *131*, 615.
- (44) Krishnan, M.; Smith, J. C. *J. Am. Chem. Soc.* **2009**, *131*, 10083.
- (45) Howard, D. L.; Kjaergaard, H. G. *Phys. Chem. Chem. Phys.* **2008**, *10*, 4113.
- (46) Manning, G. S. *Q. Rev. Biophys.* **1978**, *11*, 179.
- (47) Record, M. T.; Anderson, C. F.; Lohman, T. M. *Q. Rev. Biophys.* **1978**, *11*, 103.
- (48) Karlslake, C.; Botuyan, M. V.; Gorenstein, D. G. *Biochemistry* **1992**, *31*, 1849.
- (49) Iwahara, J.; Zweckstetter, M.; Clore, G. M. *Proc. Natl. Acad. Sci. U.S.A.* **2006**, *103*, 15062.
- (50) Blainey, P. C.; Luo, G.; Kou, S. C.; Mangel, W. F.; Verdine, G. L.; Bagchi, B.; Xie, X. S. *Nat. Struct. Mol. Biol.* **2009**, *16*, 1224.
- (51) Gorman, J.; Greene, E. C. *Nat. Struct. Mol. Biol.* **2008**, *15*, 768.
- (52) Lehmann, M. S.; Koetzle, T. F.; Hamilton, W. C. *J. Am. Chem. Soc.* **1971**, *94*, 2657.